Journal of Sound and Vibration (1997) **201**(2), 205–233

COMPLEX ENVELOPE DISPLACEMENT ANALYSIS: A QUASI-STATIC APPROACH TO VIBRATIONS

A. Carcaterra and A. Sestieri

Dipartimento di Meccanica e Aeronautica, Università "La Sapienza", 00184 Rome, Italy

(*Received* 14 *March* 1996, *and in final form* 5 *September* 1996)

A new model to analyze high frequency vibrations is presented. Instead of using the physical oscillating displacement, the problem is described in terms of a complex envelope, generated by an appropriate use of the Hilbert transform. The model can be put in the category of those methods that try to describe some representative characteristic of the oscillating solution (average energy level, thermal trend, etc.) rather than the solution itself, avoiding the computational problems connected with high frequency problems. Although the envelope solution, by itself, is sufficient and convenient to deal with structural–acoustic coupling, the proposed model presents the twofold advantage of avoiding computational problems connected with high frequency vibrations while keeping the capability of recovering the oscillating response, when required.

1. INTRODUCTION

Interest in new formulations of vibro-acoustic problems is turning increasingly to the medium and high frequency ranges, necessary to analyze and control technical problems from the design stage, to predict the energy transmission characteristics of structures and estimate the relative efficiency of different paths in a complex system. In part, this can be attributed to the development and acceptability of efficient numerical techniques that can be used reliably to solve typical low frequency structural problems; in part it is due to the design, in the aeronautical and aerospace industries, of light structures, to their interaction with the surrounding fluid, and to the increasing power of jet engines, characterized by broadband excitation; and in part it is due to the increasing attention paid by the civil community to acoustic pollution, that requires the development of more efficient prediction of the noise radiated by vibrating structures, especially in the high frequency range where the traditional formulations meet severe limitation. In fact, high frequencies mean short characteristic wavelengths, so that the traditional deterministic techniques, such as finite elements and boundary elements, are impelled to use very fine discretization meshes, with consequent prohibitive computational costs. On the other hand, the only high frequency technique proposed since the beginning of the 1960s, Statistical Energy Analysis (SEA), that has the paramount merit of being able to describe the statistical behaviour of a set of similar structures at vibro-acoustic frequencies, is still trying to receive general acceptability, its results being very case dependent. Actually, the recent research on SEA splits into two main directions: on one side a considerable effort is being put on the possibility of controlling *a priori* whether a particular system can satisfy the basic requirement of SEA (weak coupling among subsystems) [1–3] which would yield an acceptable SEA solution, and on re-formulating some basic SEA concepts [4–7]; a second

0022–460X/97/120205 + 29 $25.00/0/sv960748

direction is towards the application of traditional techniques to evaluate the classical SEA parameters (loss factors, coupling loss factors and modal density) [8].

Other new energy formulations, inspired by SEA, have been proposed since the end of the 1970s, although they attracted scientific interest from the beginning of the 1990s only. These formulations are known as thermal methods, and try to extend the basic principles of SEA, valid for finite subsystems (or for systems equipped with modes), into differential terms [9–12]. Most of the thermal methods, as others previously, have been developed, to date, for longitudinal and flexural one-dimensional systems. The important advantage of these formulations is the possibility of describing the variation of the response along the system, covering, possibly, the medium frequency gap between deterministic and statistical approaches. A frequency bandwidth exists, in fact, in which the application of classical finite elements and boundary element methods become computationally prohibitive, while, on the contrary, the modal densities of the SEA subsystems are too low to provide significant SEA results.

However, despite the considerable effort made during these years, the problem is still far from a definite and efficient solution.

Other procedures, aimed at the same goal as the thermal methods, propose contributions in a different direction, trying to overcome [13] or refusing the thermal analogy [14]. The General Energy Formulation (GEF) and its simplified version, the Smooth Energy Formulation (SEF), describe the balance between the active and reactive energy flows in a system: the SEF still provides an approximate thermal balance equation for one-dimensional systems, but fails to achieve this for more complex structures [15, 16].

In the models developed by Carcaterra and Sestieri, one attempts to describe the envelope trend of some field variable (energy or displacement), transforming the oscillating solution governed, in the frequency domain, by the Helmholtz equation, into a smooth solution. The envelope is obtained by an appropriate use of the Hilbert transform, which removes the oscillating part of the solution, although keeping its main trend along the structure.

In the attempt to circumvent some drawbacks in the problem formulation, three different envelope models have successively been developed.

In the first one, the envelope energy model (EEM) [17], only the envelope kinetic energy was used: although the model was able to recover the energy trend, and a simple linear governing equation was determined, it was not capable of describing some typical energy jumps at discontinuity points, so that, as in the thermal problems, it was necessary to utilize other techniques to estimate transmission and reflection coefficients that are required to model assembled structures. Moreover, the forcing term in the governing equation is a function of the input power. This quantity, dependent on both the excitation force and the physical velocity, is never known before the solution is available, so that an estimate of it is required. At high frequencies, it is possible to yield a sufficiently accurate estimation of the input power, because the actual system velocity can be replaced by the corresponding velocity of the infinite system. However, at low and medium frequencies, the response of the finite system differs greatly from the response of the infinite one, due to its resonant behaviour.

Therefore, a second envelope model was developed, that considered, together with the envelope energy, the displacement phase: the model was called the Envelope-PHase Energy Model (EPHEM) [18]. With this model the problem related to the energy jumps at discontinuites is completely solved. However, for flexural beams, some approximations were introduced to avoid coupling and non-linearities of the envelope and phase equations: although the extension to more complex structures was never performed, it is very apparent

that this extension would noticeably complicate the model equations. Furthermore, the input power was still the excitation term of the equations, with obvious limitations.

Consequently, a last and final model was introduced, for which a different point of view is used, although the envelope concept is still maintained: the model is called the Complex Envelope Displacement, and its application Complex Envelope Displacement Analysis (CEDA) [19, 20].

The basic idea of this formulation consists of defining a new field descriptor, related to the physical displacement by a one-to-one correspondence, that has the property, under certain conditions, that most of its energy is concentrated in the low wavenumber region. While, *per se*, this approach could be considered a re-formulation of dynamic problems, leading to interesting developments in vibro-acoustics, the opportunity for a coarse discretized numerical solution for the coresponding governing equation is also provided, which is attractive, if not fundamental, in the high frequency range.

2. GENERAL FORMULATION OF THE COMPLEX ENVELOPE DISPLACEMENT MODEL

2.1. BASIC DEFINITIONS

The complex envelope displacement theory relies on a suitable variable transformation. Consider the equation of motion for a general one-dimensional undamped structure,

$$\mathbf{L}[w(x)] + m\omega_0^2 w(x) = p(x), \tag{1}$$

$\mathbf{L}$ being a self-adjoint differential operator, $w(x)$ the displacement and $p(x)$ the external load, here assumed to be harmonic in time with frequency ω_0, implying that the steady response of the structure is also harmonic with the same frequency, so that the time variable is removed from both sides of equation (1). m is the mass per unit length of the structure.

The complex envelope displacement $\tilde{w}$ can be introduced through the action of an envelope operator $\mathbf{E}$ on the displacement w, defined as

$$\mathbf{E}(\cdot) = [\mathbf{I}(\cdot) + \mathrm{j}\mathbf{H}(\cdot)]\,\mathrm{e}^{-\mathrm{j}k_0 x}, \tag{2}$$

where $\mathbf{H}$ and $\mathbf{I}$ are the Hilbert and identity transformations, respectively, $k_0 = \omega_0/c_0$ is the carrier wavenumber, corresponding to the excitation frequency, and c_0 is the phase wave speed in the system considered. (The reason for the left arrow adopted to represent the complex envelope displacement will be better understood later on in the paper; in fact, it will be shown that the envelope displacement is obtained by shifting a wavenumber spectrum to the left toward the origin of axes.)

The Hilbert transform of a function $f(x)$ is given by [22]

$$\mathbf{H}[f(x)] = \tilde{f}(x) = \mathrm{p.v.} \int_{-\infty}^{\infty} \frac{\mathrm{f}(\xi)}{\pi(x-\xi)}\,\mathrm{d}\xi.$$

For the new variable—complex envelope displacement—one has the relationship

$$\tilde{w} = \mathbf{E}[w] = [w + \mathrm{j}\tilde{w}]\,\mathrm{e}^{-\mathrm{j}k_0 x} = \hat{w}\,\mathrm{e}^{-\mathrm{j}k_0 x}, \tag{3}$$

where $\hat{w}$ is the analytic displacement $\hat{w} = w + \mathrm{j}\tilde{w}$, and j is the imaginary unit $\sqrt{-1}$.

For the envelope operator and the complex envelope displacement, the following properties can be demonstrated.

E admits an inverse: that is,

$$\mathbf{E}(\cdot)^{-1} = \mathrm{Re}\,[(\cdot)\,\mathrm{e}^{\mathrm{j}k_0 x}].$$

This relationship permits one to recover the physical displacement once the complex envelope has been determined. In fact,

$$w(x) = \mathbf{E}^{-1}[\hat{w}] = \mathrm{Re}\,\{\hat{w}(x)\,\mathrm{e}^{\mathrm{j}k_0 x}\}. \tag{4}$$

It can be easily verified that, if the physical displacement spectrum is band limited around the carrier wavenumber k_0, the complex envelope displacement is band limited around the wavenumbers' origin. In fact, for a band-limited spectrum around k_0, the Fourier transform $W(x)$ of the physical displacement is concentrated within two limited regions around k_0 and $-k_0$ of bandwith Δk (see Figure 1(a)). It will be shown later that, in many cases of practical interest the above condition of band-limited spectrum is satisfied. The Fourier transform $\mathscr{F}$ of the analytic displacement $\hat{w}(x)$ is then given by

$$\mathscr{F}[\hat{w}] = \widehat{W}(k) = W(k) + \mathrm{j}\mathscr{F}[w(x) * 1/\pi x],$$

where the asterisk denotes convolution. Since $\mathscr{F}[1/\pi x] = -\mathrm{j}\,\mathrm{sign}\,(k)$, it follows that

$$\widehat{W}(k) = W(k) + \mathrm{sign}\,(k)W(k):$$

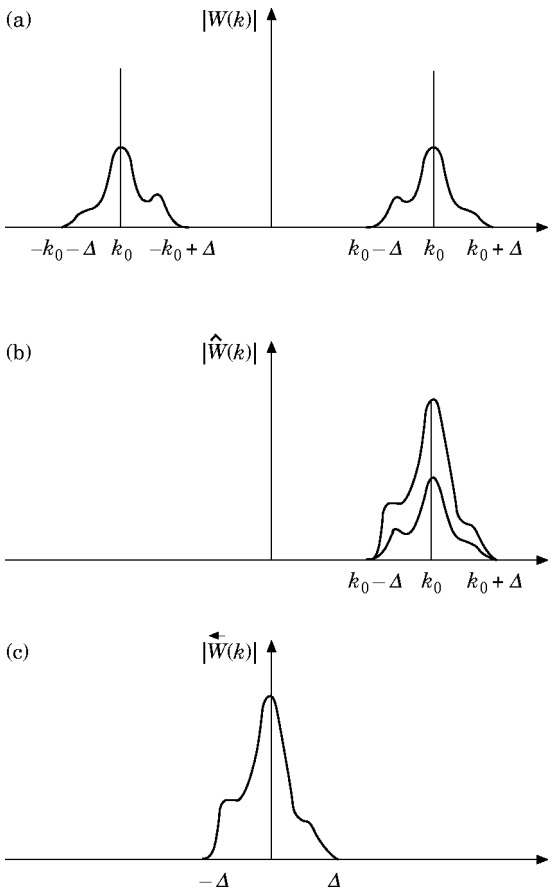

Figure 1. Fourier transforms. (a) Physical displacement; (b) analytical displacement; (c) complex envelope displacement.

i.e., the negative wavenumber contribution of $W(k)$ is deleted, and the positive one is doubled (see Figure 1(b)). Finally, the Fourier transform of the complex envelope displacement is simply expressed (see equation (3)) by $\tilde{W}(k) = \widehat{W}(k + k_0)$, corresponding to a shift of the positive wavenumber contribution of $\widehat{W}(k)$ towards the origin of wavenumbers (see Figure 1(c)). This last property indicates that the complex envelope displacement is a low wavenumber function, the correct spatial evolution of which can be described by using a limited number of samples, according to the Nyquist criterion. The sampling theorem suggests, in fact, that a correct representation of the signal can be obtained provided that the sampling frequency (wavenumber) is greater than twice the maximum frequency (wavenumber) of the signal.

One can summarize these important results. The description of the physical displacement needs a space sampling that increases with the excitation frequency ω_0, in that the sampling wavenumber is directly related to it. On the contrary, for the complex envelope displacement the space sampling is independent of ω_0 because it is proportional to the signal bandwith Δk. Consequently, the chance of describing the dynamic response of the structure by a coarse set of sampled points is obtained by keeping the same information content, even for high frequency excitation forces. The physical displacement, rapidly oscillating in space, is transformed first into a slowly oscillating signal through the complex envelope, and the solution of the dynamic problem is obtained in terms of this new variable; then, if required, an inverse transformation can be used to re-obtain the physical oscillating solution, at the low cost of interpolating the envelope displacement (see section 4).

To achieve the previous goal, a suitable governing equation in terms of the complex envelope must be solved. In the following section, this equation is determined.

2.2. COMPLEX ENVELOPE EQUATION

2.2.1. *Narrow-band displacement spectrum: basic envelope operator*

For a narrow-band displacement spectrum, the properties described in section 2.1 hold, and the complex envelope governing equation can be determined directly by applying the envelope operator to both sides of the equation of motion (1) (a different derivation is described in Appendix A):

$$\mathbf{E}\{\mathbf{L}[w]\} + m\omega_0^2\mathbf{E}\{w\} = \mathbf{E}\{p\} = \tilde{p}(x).$$

Expressing the physical displacement in terms of the complex envelope, by the inverse envelope operator, one obtains

$$\mathbf{ELE}^{-1}\{\tilde{w}(x)\} + m\omega_0^2\tilde{w} = \tilde{p}(x):$$

that is,

$$\tilde{\mathbf{L}}[\tilde{w}] + m\omega_0^2\tilde{w} = \tilde{p} = (p + \tilde{p})\,\mathrm{e}^{-\mathrm{j}k_0x}, \tag{5}$$

where a new complex envelope operator is introduced, as

$$\tilde{\mathbf{L}} = \mathbf{ELE}^{-1}. \tag{6}$$

The complex envelope equation is analogous to the original displacement equation provided that the physical displacement, the external load and the structural operator are replaced by the correspondent complex envelope terms.

2.2.2. *Wide-band displacement spectrum: general bandwidth decomposition technique*

When the displacement spectrum is not narrow, a bandwidth decomposition technique can be developed to obtain an envelope solution that still presents a significant numerical benefit. The basic idea relies on the decomposition of the actual displacement spectrum of bandwidth Δk, centered around k_0, into sub-band components of smaller width δk, followed by a translation of each sub-band toward the origin of the k's. By this technique, a set of sub-problems of small bandwidth size can be solved, which is computationally more convenient than the solution of the original physical problem.

To this aim, recalling the spectral characteristic of the analytic signal (section 2.1), divide the bandwith spectrum Δk of the analytic displacement into M sub-bands of amplitude δk. The nth spectral component of the analytic displacement spectrum $\widehat{W}_n(k)$ is put equal to the following:

$$\widehat{W}_n(k) =$$

$$\left\{ \begin{array}{ll} \widehat{W}1s(k) & \text{for} \left[k_0 - \dfrac{\Delta k}{2} + n\,\delta k \right] < k < \left[k_0 - \dfrac{\Delta k}{2} + (n+1) \right] \delta k, \quad n = 0, 1, \ldots, (N-1) \\ 0 & \text{elsewhere} \end{array} \right\}.$$

Now it is possible to apply the described envelope displacement procedure to each of the spectral components.

To produce the related governing equation for each component, a formal development is necessary. The nth spectral component of the analytic displacement is generated by multiplying the original displacement spectrum $\widehat{W}(k)$ by a rectangular window $G_n(k)$ centered around $[k_0 - \Delta k/2 + (n + 1/2)\,\delta k]$: i.e., $\widehat{W}_n(k) = W(k)G_n(k)$. The inverse Fourier transform of $\widehat{W}_n(k)$ provides the nth spatial analytic displacement:

$$\hat{w}_n(x) = \int_{-\infty}^{+\infty} w(\xi) g_n(\xi - x)\, \mathrm{d}\xi = w * g_n,$$

where

$$g_n(x) = \mathscr{F}^{-1}\{G_n(k)\} = 2\pi\,\delta k\, \sin(\delta k x/2)/(\delta k x/2).$$

A set of decomposition operators $\mathbf{D}_n$ can be introduced:

$$\mathbf{D}_n(\cdot) = \int_{-\infty}^{\infty} (\cdot) g_n(\xi - x)\, \mathrm{d}\xi = (\cdot) * g_n \qquad \text{such that } \hat{w}_n = \mathbf{D}_n(w).$$

Now the nth component of the complex envelope can be obtained by translating each generating function $\widehat{W}_n(k)$ towards the origin of the k-axis, thus obtaining

$$\tilde{W}_n(k) = \widehat{W}_n(k + k_n) = W(k + k_n) G_n(k + k_n),$$

from which the following relationship is determined:

$$\tilde{w}_n(x) = \hat{w}_n(x)\, \mathrm{e}^{-\mathrm{j}k_n x} = \mathbf{D}_n(w)\, \mathrm{e}^{-\mathrm{j}k_n x}.$$

Applying the decomposition operator to both sides of equation (1), one obtains

$$\mathbf{D}_n[\mathbf{L}(w)] + m\omega_0^2\mathbf{D}_n[w] = \mathbf{D}_n[p]$$
$$\Rightarrow \mathbf{L}[\mathbf{D}_n(w)] + m\omega_0^2\mathbf{D}_n(w) = \mathbf{D}_n(p) \Rightarrow \mathbf{L}(\hat{w}_n) + m\omega_0^2\hat{w}_n = \hat{p}_n,$$

the last step being possible because of the commutation property between the decomposition and structural operators. Proceeding as in Appendix A from equation (A2) and substituting $\hat{w}_n = \tilde{w}\,\mathrm{e}^{\mathrm{j}k_n x}$, one finally has

$$\tilde{\mathbf{L}}_n(\tilde{w}_n) + m\omega_0^2\tilde{w}_n = \tilde{p}_n, \tag{7}$$

representing the new complex envelope for the nth component. The general solution is available when the whole set M of differential equations has been solved. The numerical enhancement achieved by this procedure is discussed in section 4.

In order to reconstruct the physical solution, each of the $\tilde{W}_n(k)$ spectra, concentrated around the ks' origin, must be conveniently relocated in its proper position over the k-axis, shifting $\tilde{W}_n(k)$ on k_n towards the positive ks' direction. In this way the nth spectral component of the analytic signal, $\hat{w}_n(x)$, is correctly determined, and the complete analytic solution in the wavenumber domain is obtained as

$$\widehat{W}(k) = \sum_{n=1}^{M} \tilde{W}_n(k - k_n).$$

Transforming back into the space domain one finally has

$$\hat{w}(x) = \sum_{n=1}^{M} \tilde{w}_n(x)\,\mathrm{e}^{\mathrm{j}k_n x},$$

so that the physical displacement is easily recovered:

$$w(x) = \mathrm{Re}\,\{\hat{w}(x)\} = \sum_{n=1}^{M} \mathrm{Re}\,\{\tilde{w}_n(x)\,\mathrm{e}^{+\mathrm{j}k_n x}\}. \tag{8}$$

2.2.3. *Boundary and continuity conditions*

The existence of the inverse transformation (4) yields a straighforward derivation of the boundary conditions that must be imposed on the envelope equation.

Usually, the physical boundary conditions can be formally expressed through a suitable differential operator $\mathbf{B}$, the order and number of components of which depend on the particular problem. In general, it is $\underline{\mathbf{B}}_{(0,L)}(w) = 0$, where L is the length of the one-dimensional system. Equation (4), $w(x) = \mathbf{E}^{-1}[\tilde{w}(x)]$, relating the physical to the complex envelope displacement, leads directly to the boundary conditions of the envelope problem: i.e.,

$$\underline{\mathbf{B}}_{(0,L)}\mathbf{E}^{-1}(\tilde{w}) = 0. \tag{9}$$

Although some arguments related to the existence of spurious solutions will be discussed later, this approach establishes a complete formulation of the envelope problem.

Similar considerations can be introduced for the continuity conditions that must be imposed when assembling structures together. A general form for the continuity conditions at a joint is given by $\underline{\mathbf{C}}_{J_+}(w) = \underline{\mathbf{C}}_{J_-}(w)$, where $\underline{\mathbf{C}}$ is a suitable operator, J is the joint location, and $+$ and $-$ represent the right and left ends of the joint. The inverse transformation

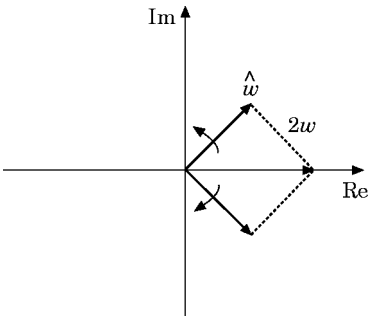

Figure 2. Integral contributions of the physical displacement in the complex plane.

allows, as for the boundary conditions, an immediate derivation of the continuity conditions for the envelope problem, as follows:

$$\underset{\sim}{\mathbf{C}}_{J_+}\mathbf{E}^{-1}(\tilde{w}) = \underset{\sim}{\mathbf{C}}_{J_-}\mathbf{E}^{-1}\{\tilde{w}\}. \tag{10}$$

At this stage it is possible to summarize the main steps of the complex envelope displacement analysis as follows: calculation of the envelope displacement $\tilde{w}$ by solving equation (5) (or (6)) with related boundary and continuity conditions (9) and (10), using a low number of sampling points; reconstruction of the physical solution by means of the inverse envelope operator (4) (or (7)).

2.3. GEOMETRICAL REPRESENTATION OF THE ENVELOPE SOLUTION

In this section the previously mentioned basic property of the envelope operator $\mathbf{E}$ is reconsidered from a geometrical point of view. The envelope operator maps the physical into the complex envelope displacement. If the band-limitedness hypothesis on the physical displacement holds, then the new variable $\tilde{w}$ is a smoother function, implying the possibility of a lower spatial sampling.

For an undamped system, w is a real function and its spectrum is symmetric around the origin, i.e., $W(k) = W^*(-k)$, so that one can write the displacement decomposition as

$$w(x) = \frac{1}{2\pi}\int_0^\infty W(k)\,\mathrm{e}^{\mathrm{j}kx}\,\mathrm{d}k + \frac{1}{2\pi}\int_0^\infty W^*(k)\,\mathrm{e}^{-\mathrm{j}kx}\,\mathrm{d}k.$$

The two integral contributions can be represented in the complex plane by a couple of counter-clockwise and clockwise rotating vectors, the sum of which is twice the amplitude of the physical displacement; see Figure 2. It can easily be proved that

$$\hat{w} = \frac{1}{\pi}\int_0^\infty W(k)\,\mathrm{e}^{\mathrm{j}kx}\,\mathrm{d}k$$

and the geometrical meaning of the analytic displacement is apparent.

Now consider the representation of the complex envelope displacement in terms of the analytic one (equation (3)):

$$\tilde{w} = \hat{w}\,\mathrm{e}^{-\mathrm{j}k_0x} \Rightarrow \begin{Bmatrix}\mathrm{Re}\,[\tilde{w}]\\ \mathrm{Im}\,[\tilde{w}]\end{Bmatrix} = \begin{bmatrix}\cos k_0x & \sin k_0x\\ -\sin k_0x & \cos k_0x\end{bmatrix}\begin{Bmatrix}\mathrm{Re}\,[\hat{w}]\\ \mathrm{Im}\,[\hat{w}]\end{Bmatrix}.$$

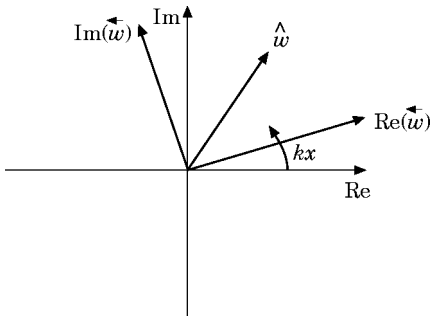

Figure 3. The real and imaginary parts of the complex envelope displacement as projections of the analytical displacement on the axes of a moving reference system.

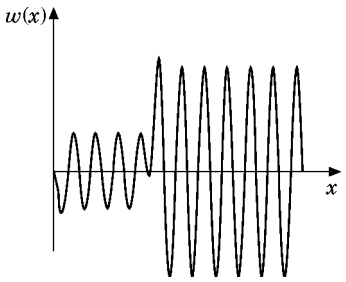

Figure 4. The displacement of a beam subjected to a concentrated load.

The matrix here is a rotation in the complex plane; hence both the analytic and complex envelope displacements are represented by the same rotating vector, the real and the imaginary components of which are referred to two different reference systems. In fact, the real and imaginary parts of $\tilde{w}$ are the projections of $\hat{w}$ on the axes of a moving reference system rotating around the origin of the complex plane at constant angular speed k_0 (see Figure 3).

If the spectrum of the displacement is concentrated around the carrier wavenumber k_0, then the rotating vector associated with $\hat{w}$ rotates at an angular speed slowly varying around the value k_0. Thus, if the components of this vector are referred to the moving reference system rotating at the constant angular speed of the carrier wavenumber k_0, then these components are slowly varying functions of the x co-ordinate. In Figures 4 and 5 the physical displacement of a beam subjected to a concentrated force and the associated real and imaginary components of the complex envelope displacement are plotted, respectively. The smooth characteristic trend of the complex envelope with respect to the rapidly oscillating trend exhibited by the physical displacement is very clear. In Figure 6

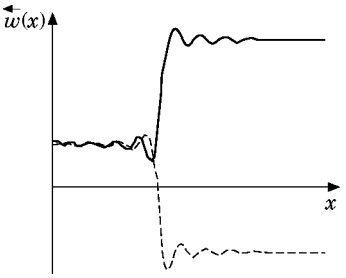

Figure 5. The real (– – – –)and imaginary (——) components of the complex envelope displacement.

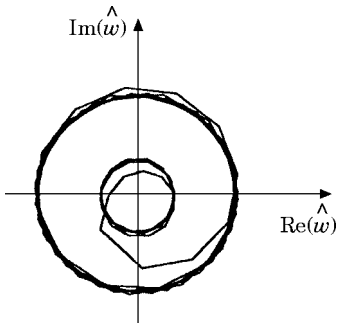

Figure 6. The analytic displacement on the complex plane.

the corresponding analytic displacement in the complex plane is shown, while in Figure 7 the plot of the complex envelope in the rotating reference frame is considered. One can observe how the two orbits described by the analytic displacement are mapped by the envelope operator into two very small regions almost collapsing into two single points. (They correspond to two vibrational energy levels along the beam.) This result confirms the "quasi-static" nature of the complex envelope representation of the dynamic structural response.

3. ENVELOPE OPERATORS FOR STRUCTURAL PROBLEMS

Due to problems related to an arising spurious solution in the envelope equation (see section 3.1.3), the envelope operators have been presently developed for one-dimensional problems (logitudinal and flexural). Here they are given explicitly for particular models of flexural beams.

3.1. EULER–BERNOULLI BEAM

For the flexural vibrations of uniform beams excited by a time-harmonic distributed load $p(x)$, the structural operator is given by $\mathbf{L}(\cdot) = \mathrm{d}^4(\cdot)/\mathrm{d}x^4$. By applying equation (6), or the procedure explained in Appendix A, the corresponding form of the structural envelope operator is determined:

$$\tilde{\mathbf{L}}(\cdot) = \mathrm{d}^4(\cdot)/\mathrm{d}x^4 + 4\mathrm{j}k_0\,\mathrm{d}^3(\cdot)/\mathrm{d}x^3 - 6k_0^2\,\mathrm{d}^2(\cdot)/\mathrm{d}x^2 - 4\mathrm{j}k_0^3\,\mathrm{d}(\cdot)/\mathrm{d}x + k_0^4(\cdot). \tag{11}$$

The fourth order envelope equation so obtained presents some difficulty in obtaining explicitly related boundary conditions.

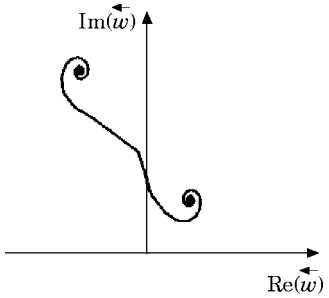

Figure 7. The complex envelope displacement in the rotating reference frame.

To overcome this problem, it is very useful to use an approximate approach proposed by Langley [21]. Langley's technique applies to concentrated loads, thus not covering the whole set of forcing excitations. However, several problems of practical interest present this type of load and, in these cases, the approximate solution is straightforward and computationally convenient. In general cases, it is necessary to solve the fourth order equation, determining the boundary conditions of the fourth order envelope problem.

3.1.1. *Reduced far field equation by Langley's approach*

In Langley's approach, valid for high frequency vibrations and for concentrated loads, the fourth order equation of the flexural problem is transformed into a second order equation accounting for the far field contributions only. However, in this case it is necessary to determine suitable boundary and joint conditions that must be imposed on the far field components only.

The differential equation of flexural beams excited by a harmonic point force is

$$\mathbf{L}_d(w) = [\mathrm{d}^4/\mathrm{d}x^4 - k_0^4](w) = (p_0/EI)\delta(x - x_F).$$

The self-adjoint differential operator $\mathbf{L}_d$ can be factorized to yield, for the homogeneous problem, a pair of far field (*ff*) and near field (*nf*) equations,

$$w_{ff} + k_0^2 w_{ff} = 0, \qquad w_{nf} - k_0^2 w_{nf} = 0,$$

the solutions of which are

$$w_{ff} = A\ \mathrm{e}^{\mathrm{j}k_0 x} + B\ \mathrm{e}^{-\mathrm{j}k_0 x}, \qquad w_{nf} = C\ \mathrm{e}^{k_0 x} + D\ \mathrm{e}^{-k_0 x}.$$

In the proximity of a constraint, provided that the vibration frequency is high enough, one of the contributions of the near field solution can usually be neglected: e.g., in $x = 0$, the second near field solution can be omitted with respect to the first one, while the first one can be cancelled at the other constraint.

Then the approximate expression of the near field is written as

$$w_{nf} = g\ \mathrm{e}^{\pm k_0 x} = g\ \mathrm{e}^{\lambda x} \Rightarrow w'_{nf} = \lambda w_{nf},$$

where $\lambda = \pm k_0$, the sign depending on the neglected near field contribution, and g is a constant denoting the coefficients C or D. Therefore, in the proximity of any constraint, the near field can be approximated as shown above to give, for the complete solution and its derivatives up to the third order,

$$w = w_{ff} + w_{nf}, \qquad w' = w'_{ff} + \lambda w_{nf},$$
$$w'' = k_0^2(w_{nf} - w_{ff}), \qquad w''' = k_0^2(\lambda w_{nf} - w'_{ff}).$$

The boundary conditions for a flexural beam are two for each end. By expressing them through the previous relationships, two equations in w_{ff}, w'_{ff} and w_{nf} are obtained. Consequently, it is possible to combine the two equations such that the near field component is eliminated and a unique condition is obtained for each end in terms of the far field component and its derivative only. This is the new condition that, together with the second one at the other end, solves the second order equation in w_{ff}.

In the same way, the continuity conditions for coupled beams can be obtained: the four continuity conditions, linearly combined two by two, yield two joint relations in the propagating component alone. Therefore, by using Langley's procedure, the flexural vibrations of each beam can be described by the second order far field equation,

$$w'' + k_0^2 w = q, \tag{12}$$

where, for the sake of simplicity, w denotes w_{ff} and (see reference [21]), $q = -p(x)/2EIk_0^2$, with $p(x) = p_0\delta(x - x_F)$ being the physical load.

The corresponding complex envelope equation, obtained in Appendix B, is given by

$$\tilde{w}'' + 2jk_0\tilde{w}' = \tilde{q} = (q + j\tilde{q})\,e^{-jk_0x}, \tag{13}$$

formally identical to the corresponding envelope equation for longitudinal vibrations [19].

Although, for the reasons previously discussed, this equation admits a smooth solution, the forcing term $\tilde{q}$ is very steep and computationally troublesome. Therefore it is convenient to integrate that equation to make the load more smooth and reach a first order formulation. This new equation is

$$\tilde{w}' + 2jk_0\tilde{w} = \int \tilde{q}\,dx, \tag{14}$$

where $\int \tilde{q}\,dx$ is a primitive of $\tilde{q}$.

3.1.2. *Complex envelope bandwidth in the wavenumber domain*

The bandwidth of the second order equation solution is here determined to verify under which conditions its wavenumber spectrum is band limited around the carrier wavenumber k_0. To this end, consider again the second order far field equation of a flexural beam excited by a time harmonic load $q(x)$ (equation (12)). As is known, its general solution is the sum of particular solution and the solution of the homogeneous equation.

The solution of the homogeneous equation is

$$w_h(x) = A_1 \cos k_0x + B_1 \sin k_0x$$

and its Fourier transform is

$$W_h(k) = \tfrac{1}{2}(A_1 + B_1/j)\delta(k - k_0) + \tfrac{1}{2}(A_1 - B_1/j)\delta(k + k_0):$$

i.e., it is entirely concentrated in k_0.

The Fourier transform of the particular solution is simply $W_p(k) = Q(k)/(k_0^2 - k^2)$ and its bandwidth depends obviously on the bandwidth of $Q(k)$. However, if $q(x)$ is limited in space (e.g., a concentrated force), $Q(k)$ is rather flat in the wavenumber domain, whereas the denominator tends to concentrate the energy of $W_p(k)$ around k_0.

Therefore the general displacement of a rather concentrated load is band limited around the carrier wavenumber, thus providing a possible load for a straight complex envelope displacement application.

3.1.3. *Presence of spurious solutions in the complex envelope equation*

It was shown that the complex envelope displacement is a solution of the envelope equation. However, in addition to it, other "spurious" (undesired) solutions are determined.

In this section, the general solution of the envelope equation will be determined to show whether and how these spurious contributions can be eliminated.

The solution of equation (14) is obtained as the sum of a particular solution and the solution of the associated homogeneous equation, given by $\tilde{w}_h(x) = C\,e^{2jk_0x}$, where C is a complex constant. A particular solution is obtained by Fourier transforming equation (14), providing

$$\tilde{W}(k) = -\tilde{Q}(k)/k(k + 2k_0).$$

Then, the general envelope solution in the space domain is given by

$$\tilde{w}(x) = -\frac{1}{2\pi}\int_{-\infty}^{\infty} \frac{\tilde{Q}(k)}{k(k+2k_0)}\, e^{jkx}\, dk + C\, e^{2jk_0x}. \tag{15}$$

It is worthwhile to point out that the particular solution exactly corresponds to the complex envelope solution $\mathbf{E}(w)$ (Appendix C), that, as shown, is a slowly space-oscillating solution: this implies that the envelope equation guarantees the existence of $\mathbf{E}(w)$, but does not exclude other results, as does the homogeneous solution. Unfortunately, the presence of this term is troublesome, because it is a "spurious" rapidly oscillating space component (wavenumber $2k_0$), superimposed on the particular solution.

Consequently, the spurious contribution should be eliminated to solve the complex envelope equation with a low spatial resolution. To obtain this goal, equation (14) is solved with a particular boundary condition. The complex envelope displacement at $x = 0$ yields

$$\tilde{w}(0) = -\frac{1}{2}\int_{\infty}^{\infty} \frac{\tilde{Q}(k)}{k(k+2k_0)}\, dk + C. \tag{16}$$

By assuming that in it $C = 0$, equation (14), solved with this boundary condition, provides only the desired solution $\mathbf{E}(w)$, which can be determined with only a few sampled points. Once this complex envelope solution ($\tilde{w}_0(x)$) is obtained, the space solution is determined by $w_0(x) = \mathbf{E}^{-1}\{\tilde{w}_0(x)\}$, which solves the original motion equation $w_0'' + k_0^2 w_0 = p$. Nevertheless, this solution does not satisfy the boundary conditions of the problem: it represents only a particular solution of the motion equation. Therefore the complete required solution is given by

$$w(x) = w_0(x) + A\cos k_0x + B\sin k_0x, \tag{17}$$

where A and B are determined by the physical boundary conditions.

This result can be reached by a different procedure. For an equation of the same nature as equation (13), its solution is defined up to an arbitrary constant. Thus, if $\tilde{w}_0(x)$ is a solution of equation (13) (and (14)), so is $\tilde{w}_0(x) + \gamma$, being γ a complex constant. Then γ can be determined so that $\mathbf{E}^{-1}(\tilde{w}_0(x) + \gamma)$ satisfies the physical boundary conditions. Since $\gamma = \gamma_R + j\gamma_I$, there are two real constants to satisfy two boundary conditions, that explicitly provide a solution equivalent to expression (17). In fact, it is

$$\mathbf{E}^{-1}(\tilde{w}_0(x) + \gamma) = \mathrm{Re}\,\{(\tilde{w}_0(x) + \gamma)\, e^{jk_0x}\} = \mathrm{Re}\,\{\tilde{w}_0\, e^{jk_0x}\} + \gamma_R\cos k_0x - \gamma_I\sin k_0x.$$

Considering that $w_0(x) = \mathrm{Re}\,\{\tilde{w}_0\, e^{jk_0x}\}$, one has

$$w(x) = w_0(x) - \gamma_I\sin k_0x + \gamma_R\cos k_0x,$$

equivalent to solution (17) if $\gamma_R = A$ and $\gamma_I = -B$.

In conclusion, the subsequent steps of the procedure are as follows.

Solve initially the equation $\tilde{w}' + 2jk_0\tilde{w} = \int \tilde{q}\, dx$ with the condition provided by equation (16) with $C = 0$. Note that for a concentrated load $p = p_0\delta(x - x_F)$, it can be easily shown that $\tilde{w}(0) \simeq 0$, so that in practice the evaluation of expression (16) can be avoided

Determine the physical solution from

$$w(x) = \mathbf{E}^{-1}(\tilde{w}_0 + \gamma) = \mathrm{Re}\,\{(\tilde{w}_0 + \gamma)\, e^{jk_0x}\},$$

where γ is obtained by imposing the boundary conditions.

3.1.4. *Boundary and continuity conditions for flexural beams*

As discussed in section 2.2.3, the boundary conditions of the physical problem can be simply represented by a suitable differential operator $\underline{\mathbf{B}}$ that, for the flexural problem, is a third order operator involving the displacement and its derivatives up to the third order, with four components (two for each end of the beam). By using Langley's technique, the flexural problem is reduced to the second order, and the coefficients of the first order $\underline{\mathbf{B}}$ operator, with two components, can be easily calculated by applying the reduction technique previously discussed. Once the far field components of $\underline{\mathbf{B}}$ are determined, it is possible to compute the boundary conditions for the envelope equation (13). In fact, it is

$$\underline{\mathbf{B}}_{(0,L)}(w) = \underline{\mathbf{B}}_{(0,L)}[\mathbf{E}^{-1}(\tilde{w})] = \underline{\mathbf{B}}_{(0,L)}[\mathbf{E}^{-1}(\tilde{w}_0 + \gamma)] = \underline{\mathbf{B}}_{0,L}[\mathrm{Re}\,\{(\tilde{w}_0 + \gamma)\,\mathrm{e}^{\mathrm{j}k_0 x}\}] = 0,$$

where

$$\underline{\mathbf{B}}_{(0,L)} = \begin{bmatrix} b_{11}(\cdot)|_0 + b_{12}\,\mathrm{d}(\cdot)/\mathrm{d}x|_0 \\ b_{21}(\cdot)|_L + b_{22}\,\mathrm{d}(\cdot)/\mathrm{d}x|_L \end{bmatrix}.$$

A similar procedure can be applied for a joint; in this case it is possible to define a (γ_- and γ_+) for any section of beam that also involves the boundary conditions, and write

$$\underline{\mathbf{C}}_{J_-}[\mathrm{Re}\,\{(\tilde{w}_0 + \gamma_-)\,\mathrm{e}^{\mathrm{j}k_{0-}x}\}] = \underline{\mathbf{C}}_{J_+}[\mathrm{Re}\,\{(\tilde{w}_0 + \gamma_+)\,\mathrm{e}^{\mathrm{j}k_{0+}x}\}]$$

$\underline{\mathbf{C}}$ being a second order operator of the form

$$\begin{bmatrix} c_{11}(\cdot)|_J + c_{12}\mathrm{d}(\cdot)/\mathrm{d}x|_J \\ c_{21}(\cdot)|_J + c_{22}\mathrm{d}(\cdot)/\mathrm{d}x|_J \end{bmatrix}.$$

k_{0_-} and k_{0_+} account for possible different cross-sections of the assembled beams. In this way, the problem is solved completely.

3.1.5. *General fourth order equation*

The general flexural problem is characterized by both propagating waves and near field contributions. The propagating terms $\mathrm{e}^{\pm \mathrm{j}k_0 x}$ give rise, for concentrated loads, to wavenumbers' band-limited contributions around the carrier wavenumber k_0, that make the application of the complex envelope displacement approach particularly feasible. On the contrary, the presence of the evanescent near fields $\mathrm{e}^{\pm k_0 x}$ produces contributions at lower wavenumbers, thus generating a different spectral solution. In contrast with the pure propagating case, the near field contribution extends the signal bandwidth until the origin of the k-axis.

A possible technique is the bandwidth decomposition discussed in section 2.2.2, implying the solution of a similar set of equations. For the general band centered in k_n, the corresponding equation is

$$\frac{\mathrm{d}^4\tilde{w}_n}{\mathrm{d}x^4} + 4\mathrm{j}k_n\frac{\mathrm{d}^3\tilde{w}_n}{\mathrm{d}x^3} - 6k_n^2\frac{\mathrm{d}^2\tilde{w}_n}{\mathrm{d}x^2} - 4\mathrm{j}k_n^3\frac{\mathrm{d}\tilde{w}_n}{\mathrm{d}x} + (k_n^4 - k_0^4)\tilde{w} = \frac{\tilde{p}}{EI}.$$

For any of these equations, the problem of the spurious solutions related to the solution of the associated homogeneous equation must be considered. A procedure similar to the one developed in section 3.1.3 must be used to eliminate the spurious solution.

The general solution is again given by the contribution of a particular solution and the solution of the homogeneous equation. Upon using the Fourier transform, the first one yields

$$(k^4 + 4k_h k^3 - 6k_h^2 k^2 + 4k_h^3 k + k_h^4 - k_0^4)\tilde{W}_h(k) = \tilde{P}_h(k),$$

or, synthetically,

$$B_h(k)\tilde{W}_h(k) = \tilde{P}_h(k) \Rightarrow W_h(k) = \tilde{P}_h(k)/B_h(k).$$

With k_{h_r} $(r = 1, \ldots, 4)$ denoting the characteristic roots of the homogeneous equation, the general solution is then obtained as

$$\tilde{w}_h(x) = \frac{1}{2}\int_{-\infty}^{\infty} \frac{\tilde{P}_h(k)}{B_h(k)} \, \mathrm{e}^{\mathrm{j}kx} \, \mathrm{d}k + \sum_{r=1}^{4} C_{h_r} \, \mathrm{e}^{\mathrm{j}k_{h_r}x}.$$

To eliminate the spurious homogeneous solution containing rapidly oscillating contributions, it is necessary to choose suitable conditions such that $C_{h_r} \equiv 0$. They are

$$\left.\frac{\mathrm{d}^p(\tilde{w}_h)}{\mathrm{d}x^p}\right|_{x=0} = \frac{1}{2}\int_{-\infty}^{\infty} \frac{\tilde{P}_h(k)(\mathrm{j}k)^p}{B_h(k)} \, \mathrm{d}k, \qquad p = 0, \ldots, 3.$$

The $\tilde{w}_{0_h}(x)$ are obtained with these conditions, and the particular solution of the original equation of motion is determined by combining and modulating the $\tilde{w}_{0_h}$s: i.e.,

$$w_p(x) = \sum_h \mathrm{Re}\,\{\tilde{w}_{0_h}(x) \, \mathrm{e}^{\mathrm{j}k_h x}\}.$$

The whole solution is calculated by adding to it the homogeneous solution,

$$w(x) = \sum_h \mathrm{Re}\,\{\tilde{w}_{0_h}(x) \, \mathrm{e}^{\mathrm{j}k_0 x}\} + A \, \mathrm{e}^{-\mathrm{j}k_0 x} + B \, \mathrm{e}^{\mathrm{j}k_0 x} + C \, \mathrm{e}^{-k_0 x} + D \, \mathrm{e}^{k_0 x},$$

where the A, B, C and D are determined by imposing the boundary conditions on $w(x)$.

This procedure, more complicated than that developed for the second order equation, can be used for any applied load, unlike the reduced second order equation determined from Langley's approach, which can be applied only to the case of concentrated loads.

3.2. TIMOSHENKO BEAM

As the complex envelope displacement is especially useful to describe high frequency dynamic problems, it is worthwhile to extend the procedure to the Timoshenko beam model, in which the effects of rotary inertia and shear deformation are accounted for.

The Timoshenko beam equation is subjected to a time-harmonic load with frequency ω_0, is:

$$\partial^4 w/\partial x^4 + \Gamma^2 \, \partial^2 w/\partial x^2 - k_0^4 w = p \qquad \text{with } \Gamma^2 = (\rho/E)(1 + \chi E/G)\omega^2,$$

χ being the shear parameter, G the shear modulus and ρ the material density of the beam. The associatied characteristic polynomial is then $k^4 + \Gamma^2 k^2 - k_0^4 = 0$, the roots of which are

$$k_{\pm} = \pm\sqrt{\frac{-\Gamma^2 + \sqrt{\Gamma^4 + 4k_0^2}}{2}} = \pm\alpha, \qquad k_{\pm j} = \pm\mathrm{j}\sqrt{\frac{\Gamma^2 + \sqrt{\Gamma^4 + 4k_0^2}}{2}} = \pm\mathrm{j}\beta.$$

The characteristic polynomial can be factorized in the form

$$(k-\alpha)(k+\alpha)(k-\mathrm{j}\beta)(k+\mathrm{j}\beta)=0 \Rightarrow (k^2-\alpha^2)(k^2+\beta^2)=0,$$

so that the structural operator of the Timoshenko beam can be written as

$$[\partial^4(\cdot)/\partial x^4+\Gamma^4\,\partial^2(\cdot)/\partial x^2-k_0^4(\cdot)]=[\partial^2(\cdot)/\partial x^2-\alpha^2(\cdot)][\partial^2(\cdot)/\partial x^2+\beta^2(\cdot)].$$

The propagation operator associated with the Timoshenko beam, recovering the far field solution, is then

$$\mathbf{L}_p(\cdot)=\partial^2(\cdot)/\partial x^2+\beta^2(\cdot).$$

In view of the expression for β written above, one finally obtains

$$\partial^2 w/\partial x^2+k_{0T}^2 w=p,$$

$$\text{where } k_{0T}^2=\omega^2[(\zeta/c_L^2)+\sqrt{(c_B^4\zeta^2+4c_L^4)/c_L^4c_B^4}]$$

and

$$\xi=(1+\chi E)/G.$$

Therefore the complex envelope displacement analysis can be directly applied to the Timoshenko beam without relevant modifications: the derived equation corresponds to equation (13) with k_{0T} replacing k_0.

3.3. DISSIPATIVE DYNAMIC SYSTEM

The introduction of dissipative effects is not trivial.

Consider a structural damped beam. In this case Young's modulus $E_c=E(1+\mathrm{j}\eta)$ and the physical displacement in the equation of motion becomes complex. It is known that in such a case the Fourier transform of the displacement no longer exhibits a Hilbertian symmetry in the spectrum. However, it is still possible to introduce the analytic and complex envelope displacements, using for them the same formal definitions:

$$w=w_R+\mathrm{j}w_I \Rightarrow \hat{w}=w+\mathrm{j}\tilde{w}=(w_R-\tilde{w}_I)+\mathrm{j}(w_I+\tilde{w}_R),$$

$$\tilde{w}=\hat{w}\,\mathrm{e}^{-\mathrm{j}k_0x}=[(w_R-\tilde{w}_I)+\mathrm{j}(w_I+\tilde{w}_R)]\,\mathrm{e}^{-\mathrm{j}k_0x}.$$

Therefore it is straightforward to determine the complex envelope equation in the presence of damping, as made in the conservative case.

The problem arises when one tries to solve the envelope equation, because now $w\neq \mathrm{Re}\{\tilde{w}\,\mathrm{e}^{\mathrm{j}k_0x}\}$, and the boundary conditions of the envelope problem are not immediately available. This happens due to the loss of symmetry in the spectrum of the damped displacement. In fact, the application of the envelope operator produces two effects on the displacement function: the first is the cancellation of the negative wavenumber contribution in the spectrum; and the second is the shift of the spectrum towards the origin of the wavenumber axis. The first operation definitely implies a loss of information about the displacement function when the spectrum is not symmetric: hence the impossibility of performing an inverse operation, and, consequently, the loss of the one-to-one correspondence between w and $\tilde{w}$. However, there is a way to overcome the problem. By introducing a vector the components of which are the real and imaginary parts of the physical displacement, it is possible to write

$$w''+k_0^2(1-\mathrm{j}\eta)w=q \Rightarrow (w_R''+\mathrm{j}w_I'')+k_0^2(1-\mathrm{j}\eta)(w_R+\mathrm{j}w_I)=q_R+\mathrm{j}q_I.$$

By separating the real and imaginary parts and writing them in matrix form, one has

$$\begin{Bmatrix} w_R \\ w_I \end{Bmatrix}'' + k_0^2 \begin{bmatrix} 1 & \eta/2 \\ -\eta/2 & 1 \end{bmatrix} \begin{Bmatrix} w_R \\ w_I \end{Bmatrix} = \begin{Bmatrix} q_R \\ q_I \end{Bmatrix} \Rightarrow \underline{u}'' + \mathbf{P}\underline{u} = \underline{r},$$

where $\mathbf{P}$ is the above matrix and the vectors $\underline{u}$ and $\underline{r}$ are, respectively,

$$\underline{u} = \begin{Bmatrix} w_R \\ w_I \end{Bmatrix}, \qquad \underline{r} = \begin{Bmatrix} q_R \\ q_I \end{Bmatrix}.$$

By Hilbert transforming this equation, one has

$$\underline{\hat{u}}'' + \mathbf{P}\underline{\hat{u}} = \underline{\hat{r}}. \tag{18}$$

Then the complex envelope displacement vector can be introduced as

$$\underline{\check{u}} = \begin{Bmatrix} \check{u}_R \\ \check{u}_I \end{Bmatrix} = \begin{Bmatrix} \hat{u}_R \, \mathrm{e}^{-\mathrm{j}k_0 x} \\ \hat{u}_I \, \mathrm{e}^{-\mathrm{j}k_0 x} \end{Bmatrix} = \begin{bmatrix} \mathrm{e}^{-\mathrm{j}k_0 x} & 0 \\ 0 & \mathrm{e}^{-\mathrm{j}k_0 x} \end{bmatrix} \begin{Bmatrix} \hat{u}_R \\ \hat{u}_I \end{Bmatrix},$$

so that

$$\underline{\hat{u}} = [\mathbf{Exp}]\underline{\check{u}}, \qquad \text{with } \mathbf{Exp} = \begin{bmatrix} \mathrm{e}^{\mathrm{j}k_0 x} & 0 \\ 0 & \mathrm{e}^{\mathrm{j}k_0 x} \end{bmatrix}.$$

By substituting this expression into equation (18), the complex envelope displacement equation for the damped beam is obtained,

$$\underline{\check{u}}'' + 2\mathrm{j}k_0\underline{\check{u}}' + \mathbf{P}\underline{\check{u}} = \underline{\check{r}},$$

and, after integration,

$$\underline{\check{u}}' + 2\mathrm{j}k_0\underline{\check{u}} + \mathbf{P}\int \underline{\check{u}}(\xi)\,\mathrm{d}\xi = \int \underline{\check{r}}(\xi)\,\mathrm{d}\xi.$$

Then a solution technique analogous to the one made for the undamped case can be developed.

In this case it would be particularly convenient to obtain the solution by using the Fourier transform in the wavenumber domain: namely,

$$\mathrm{j}k\underline{\check{U}} + 2\mathrm{j}k_0\underline{\check{U}} + \mathbf{P}(1/\mathrm{j}k)\underline{\check{U}} = (1/\mathrm{j}k)\underline{\check{R}},$$

so that

$$\underline{\check{U}} = (1/\mathrm{j}k)[(1/\mathrm{j}k)\mathbf{P} + \mathrm{j}(k + 2k_0)\mathbf{I}]^{-1}\underline{\check{R}},$$

and thus the spatial displacement solution is

$$\underline{u} = \mathrm{Re}\,[\mathbf{Exp}\,(\mathscr{F}^{-1}\{\underline{\check{U}}\} + \underline{c})],$$

where $\underline{c}$ is a vector used to fit the boundary conditions.

Note that if the same Fourier transform technique is applied to the original equation of motion, the mesh necessary to perform the numerical integration is much finer than the one necessary to solve the complex envelope equation (see section 4.3).

4. COMPUTATIONAL PROBLEMS

4.1. HILBERT TRANSFORM OF A CONCENTRATED LOAD

In the application of the envelope method, the only quantity that must be practically determined to solve the envelope equation is the envelope input load $\mathbf{E}[q(x)]$. Specifically (see equation (4)), one must compute the integral

$$\int \mathbf{E}[q(x)]\,\mathrm{d}x = \int \tilde{q}\,\mathrm{d}x = \int (q + \mathrm{j}\tilde{q})\,\mathrm{e}^{-\mathrm{j}k_0 x}\,\mathrm{d}x.$$

This operation implies that an algorithm must be available to determine $\tilde{q}$.

The problem is sufficiently dealt with in the literature [22, 23] and different solutions are possible. Note that for some functions the Hilbert transform is known analytically. One of these cases is the concentrated load $q(x) = q_0\delta(x - x_F)$. Then, apparently, the problem should be of immediate solution because this transform is analytically available as [23]

$$\mathbf{H}\{\delta(x - x_F)\} = 1/\pi(x - x_F).$$

However, this function presents a singular point at $x = x_F$, which is also present as a forcing term in the envelope equation:

$$\int \left[\delta(x - x_F) + \mathrm{j}\,\frac{1}{\pi(x - x_F)}\right]\mathrm{e}^{-\mathrm{j}k_0 x}\,\mathrm{d}x.$$

This implies a considerable numerical difficulty. To circumvent this problem, it is convenient to use a numerical approach based on the Fourier transform to compute the Hilbert transform. In fact, the Fourier transform of a convolution is a product: i.e.,

$$\tilde{q}(x) = q(x) * 1/\pi x \Rightarrow \tilde{Q}(k) = Q(k)\mathscr{F}\{1/\pi x\} = -\mathrm{j}\ \mathrm{sign}\ (k)Q(k),$$

so that it is finally

$$\tilde{q} = \mathscr{F}^{-1}\{-\mathrm{j}\ \mathrm{sign}\ (k)Q(k)\}. \tag{19}$$

For the numerical application of this algorithm to a concentrated load $q(x) = q_0\delta(x - x_F)$, it can be convenient to approximate $q(x)$ by the function $q_a(x)$ (a Hanning window):

$$q_{\mathrm{a}}(x) = \left\{ \begin{array}{ll} \left[1 - \dfrac{\cos 2\pi(x - x_F)}{\Delta x}\right]\dfrac{q_0}{\Delta x} & \text{for} \quad x_F - \Delta x/2 < x < x_F + \Delta x/2 \\ 0 & \text{for} \quad x > |\Delta x/2| \end{array} \right\}.$$

Since $\int_0^L q(x)\,\mathrm{d}x = q_0$, provided that the condition $\Delta x \ll \lambda_0$ is fulfilled, $\lambda_0 = 2\pi/k$ being the forced wavelength on the beam, the load distribution previously defined behaves as a concentrated load. Therefore equation (19), that uses the FFT, permits one to perform the Hilbert transform of any load, including the case of concentrated forces.

4.2. RECOVERNING THE PHYSICAL RESPONSE: THE INTERPOLATION PROCEDURE

Once the envelope displacement is determined, the physical response can be reconstructed whenever required. It is necessary to remember that, due to the mentioned spectral properties, the solution of the complex envelope equation is usually obtained with a few samples; the opposite holds for the physical solution, which requires a high number of grid points.

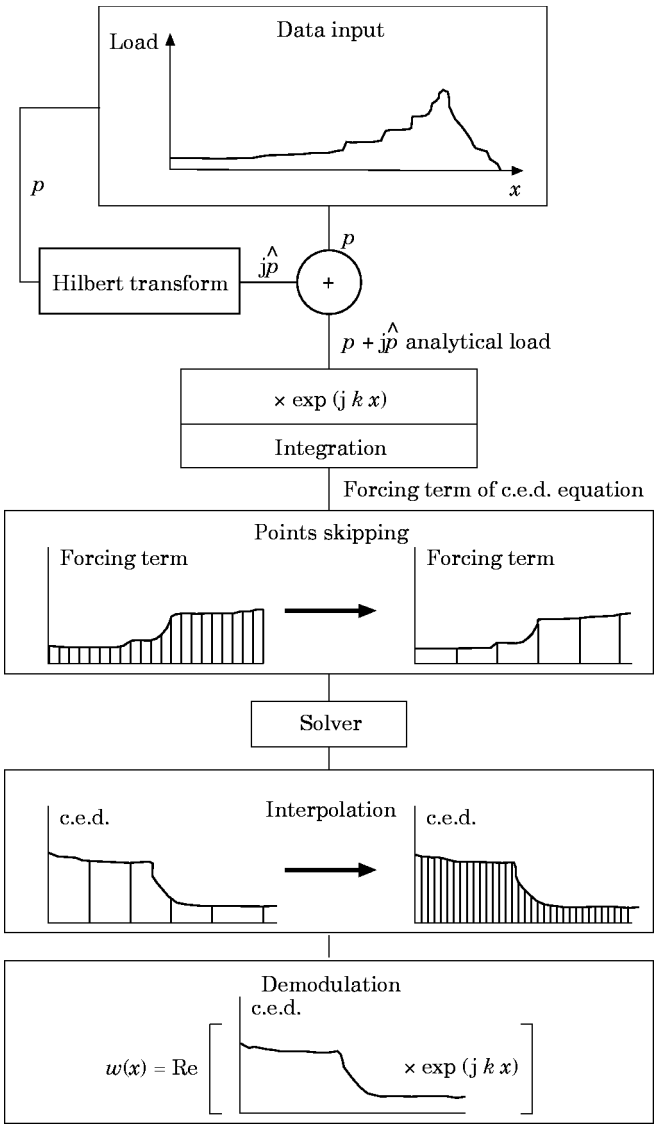

Figure 8. A block diagram to recover the physical displacement from the complex envelope displacement.

The recovering expression for the physical displacement is $w = \mathbf{E}^{-1}(\tilde{w}) = \mathrm{Re}\,\{\tilde{w}\,\mathrm{e}^{\mathrm{j}k_0 x}\}$. Then, to obtain w the complex envelope displacement must be multiplied by the complex exponential, which is very rapidly oscillating in space. More specifically, the numerical solution of $\tilde{w}$ consists of N_r values (see section 4.3); on the contrary, the complex exponential consists of N samples. Usually, $N \gg N_r$. Therefore, one has to add a suitable number of samples to the original numerical solution of the envelope displacement to recover the physical one. This can be obtained by interpolation.

Several interpolation techniques can be used: in many tests performed we verified that even a linear interpolation yields satisfactory results.

The recovery scheme is shown in the block diagram of Figure 8.

4.3. THE NUMERICAL EFFICIENCY OF THE COMPLEX ENVELOPE APPROACH

Attention is here focused on the time saving of the complex envelope displacement with respect to the physical solution.

The basic spectral properties of both the physical and envelope displacements, are as previously noted, $\mathscr{F}(w) = 0$ for $|k - k_0| > \Delta k$ and $\mathscr{F}(\tilde{w}) = 0$ for $|k| > \Delta k$. The second property implies a few considerations highlighting the numerical efficiency of the complex envelope displacement in the high frequency range. In fact, it can be argued that a correct sampling can be obtained provided that, for the physical and complex envelope displacements, the samping steps satisfy the following Nyquist limitations, respectively:

$$\Delta x \leqslant 1/2(k_0 + \Delta k), \qquad \Delta x_r \leqslant 1/2\Delta k.$$

Analogous limitations for the number of samples hold: i.e.,

$$N = L/\Delta x \geqslant 2(k_0 + \Delta k)L, \qquad N_r = L/\Delta x_r \geqslant 2\Delta k L,$$

where L is the length of the beam. By these relationships, the numerical time saving in terms of the sampled points can be expressed in the simple form $N/N_r = 1 + k_0/\Delta k$. It is also important to determine the general relationship between the computational time for both the physical and envelope displacement procedures.

The solution of a differential equation by some numerical procedures, such as the finite element or finite difference technique, leads generally to an algebraic problem, implying the calculation of an inverse matrix. The solution of a N-dimensional problem requires a computational time proportional to N^3, when using general matrix inversion algorithms such as Gauss–Jordan elimination, LU decomposition etc., that can solve the problem without any assumption about the matrix form. In this case, the ratio between the time required by a traditional procedure and by the envelope displacement technique can be simply expressed as

$$eff = \frac{T_{trad}}{T_{CEDA}} = \left(\frac{N}{N_r}\right)^3 = \left(1 + \frac{k_0}{\Delta k}\right)^3 = \left(\frac{k_0}{\Delta k}\right)^3 + 3\left(\frac{k_0}{\Delta k}\right)^2 + 3\left(\frac{k_0}{\Delta k}\right) + 1. \tag{20}$$

As is obvious, the numerical efficiency of the complex envelope displacement depends on the ratio between the value of the carrier wavenumber and the bandwidth of the displacement spectrum. When this spectrum is concentrated around the carrier wavenumber, i.e., the bandwidth is relatively small in comparison with k_0, the efficiency is very high.

When the solving matrix is sparse or banded, some specific algorithm can be conveniently employed. The simplification in this case can reduce the computational effort, and the computational time is generally proportional to a power α of the size of the problem, where $1 < \alpha < 3$. Therefore the efficiency of the complex envelope displacement algorithm depends on the order of the discretization procedure used so that the efficiency is more generally expressed by

$$eff = T_{trad}/T_{CEDA} = (N/N_r)^{\alpha} = (1 + k_0/\Delta k)^{\alpha}, \qquad 1 < \alpha < 3. \tag{21}$$

In section 3 the possibility of solving the problem directly in the wavenumber domain through the use of the Fourier transform was considered. It is well known that when using the Fast Fourier Transform (FFT) algorithm on a set of N samples, the number of

numerical computations is proportional to $N \log_2 (N)$. Then, the numerical efficiency of the envelope displacement, when the FFT technique is used, can be computed as

$$eff = \frac{N \log_2 (N)}{N_r \log_2 (N_r)} = \left(\frac{N}{N_r}\right)\left[\frac{\log_2 (N)}{\log_2 (N_r)}\right] = \left(1 + \frac{k_0}{\Delta k}\right)\left[\frac{\log_2 [2(k_0 + \Delta k)L}{\log_2 [2\Delta k L]}\right].$$

Under the assumption that $k_0/\Delta k \gg 1$, a simplified expression is obtained,

$$eff \approx (k_0/\Delta k) \log_2 (k_0), \tag{22}$$

and even in this case the numerical advantage of the complex envelope displacement analysis is apparent.

The efficiency of the complex envelope displacement when the decomposition technique presented in section 2.2.2 is used can be obtained as follows. Each equation generated in the decomposition process requires $(2\delta k L)$ sampled points, so that a computational time $(2\delta k L)^\alpha$ can be estimated. This procedure must be repeated for each spectral displacement component: i.e., $M = \Delta k/\delta k$ times. The efficiency is then

$$eff = \frac{[2(k_0 + \Delta k)L]^\alpha}{M(2\delta k L)^\alpha} = \frac{(k_0 + \Delta k)^\alpha}{(\delta k)^{\alpha - 1}\,\Delta k} = \left(1 + \frac{k_0}{\Delta k}\right)^\alpha \left\{\frac{\pi \Delta k}{\delta k}\right\}^{\alpha - 1}. \tag{23}$$

This expression is directly comparable with the one obtained from the standard envelope displacement procedure. The effect of the new factor $(\Delta k/\delta k)^{\alpha - 1}$ is evident. If $\alpha = 1$ the efficiency equals the value of the standard procedure; otherwise one has a considerable advantage as the sub-bandwidth size δk decreases. There is, of course, a limitation on the minimum acceptable size for it. In fact, the basic condition $\delta k > 1/L$ must be verified to avoid that the sampling step Δx_n of each sub-problem exceeds the length of the beam. With the limitation, the following efficiency expression is obtained:

$$eff = (1 + k_0/\Delta k)^\alpha (\Delta k L)^{\alpha - 1} = (1 + k_0/\Delta k)^\alpha (N/2)^{\alpha - 1}.$$

This shows that the numerical efficiency increases with respect to the standard complex envelope displacement analysis as the number of samples of the physical solution increases.

The possibility of a drastic reduction of samples and the related low spatial resolution make it clear that the complex envelope displacement permits a low cost numerical solution, especially in the high frequency range.

5. SIMULATED RESULTS

The following numerical simulations are presented only for the reduced second order equation obtained by Langley's procedure, which is certainly the case of major interest in practical applications. Three cases are considered of increasing difficulty.

The first example refers to two steel beams ($E = 2{\cdot}1 \times 10^{11}$ N/m^2, $\rho = 7800$ kg/m^3) of equal cross-section with hinged ends, coupled by a simple support. The characteristic dimensions of the beams and their section are shown in Figure 9.

The system is excited by two concentrated loads of amplitude $F_1 = 1000$ N and $F_2 = 500$ N, respectively, and equal frequency ($f = 12\,000$ Hz). For this case, all of the characteristic variables of the CEDA model are presented. The first operation is performed on the excitation load $F_1\delta(x - 0{\cdot}5) + F_2\delta(x - 2{\cdot}5)$. As explained in section 4.1, these loads are numerically represented by two Hanning windows located at $x = 0{\cdot}5$ and $x = 2{\cdot}5$, respectively, of amplitude $\Delta x = 0{\cdot}02$ m. It is worthwhile to point out that the wavelength corresponding to the frequency of 12 000 Hz is equal to 0·17 m. The Hilbert transform of

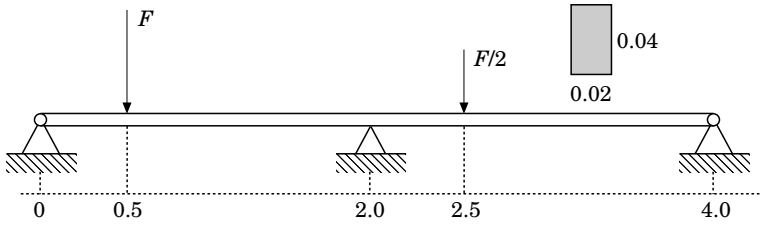

Figure 9. Simulated test 1: the dimensions of the beam.

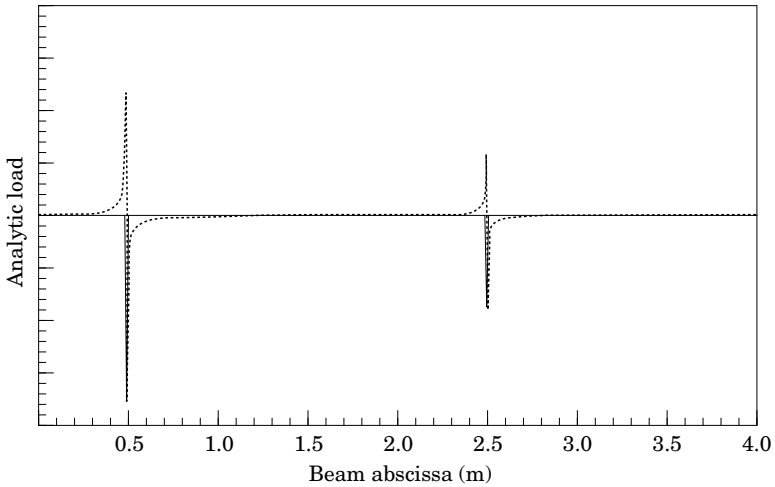

Figure 10. Test 1: the real (——) and imaginary (– – –) parts of the analytic load.

the load is computed through the Fourier transform. In Figure 10 the determined loads, p and $\hat{p}$, are considered, while in Figure 11 the real and imaginary parts of the complex envelope load $\int \check{q}\,\mathrm{d}x$ are presented. After the skipping operation (see the block diagram of Figure 8), the complex envelope load was described by 15 samples only for each beam. The envelope equation (14) was solved with this load, obtaining the solution $\tilde{w}_0$, the real

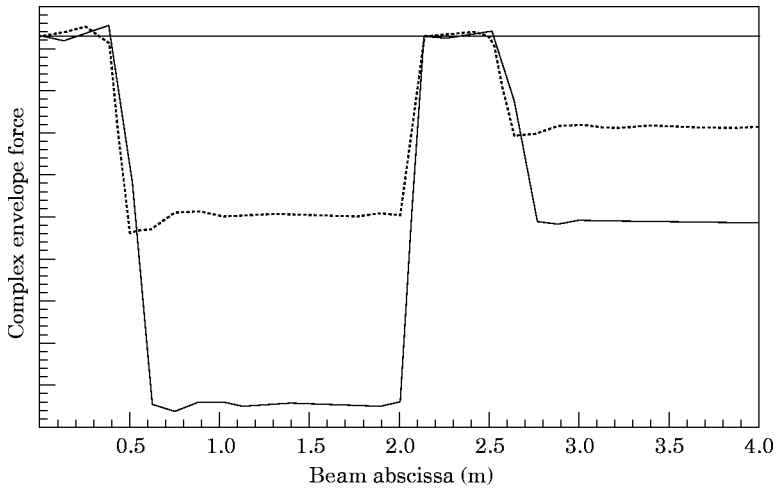

Figure 11. Test 1: the real (– – –) and imaginary (——) components of the complex envelope load.

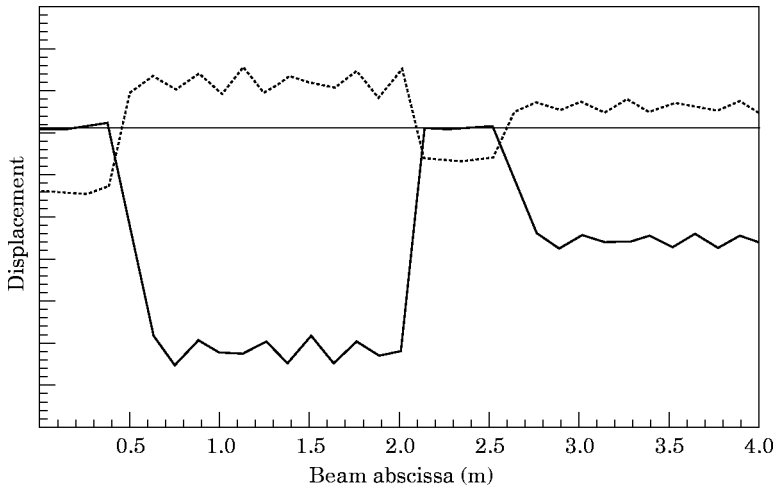

Figure 12. Test 1: the real (———) and imaginary (– – –) components of the complex envelope displacement.

and imaginary parts of which are shown in Figure 12. In Figure 13 the complex envelope displacement is considered in the complex plane (see section 2.3). At different abscissas x, the end of this complex vector moves on the complex plane towards four delimited regions, almost collapsing into a point. These points correspond to four vibro-energetic levels along the beam (see Figure 14). It is confirmed that the energetic content of $\tilde{w}_0$ is mainly concentrated at low wavenumbers. The subsequent steps concerning interpolation and demodulation lead to the physical displacement shown in Figure 14, which is compared with the exact numerical solution (obtained by a finite difference scheme, with 400 sampled points). The agreement is quite good, especially in view of the difference between the number of samples for the CEDA solution versus those of the exact one (30 versus 400).

The second case refers to the same two beams of the previous case, coupled, as before, by a simple support. The applied load consists, in this case, of two periodic forces, the amplitudes of which are $F_1 = 1000$ N and $F_2 = 500$ N respectively. The period of the two forces is the same and the force spectrum consists of two harmonics $f_1 = 12\,000$ Hz and

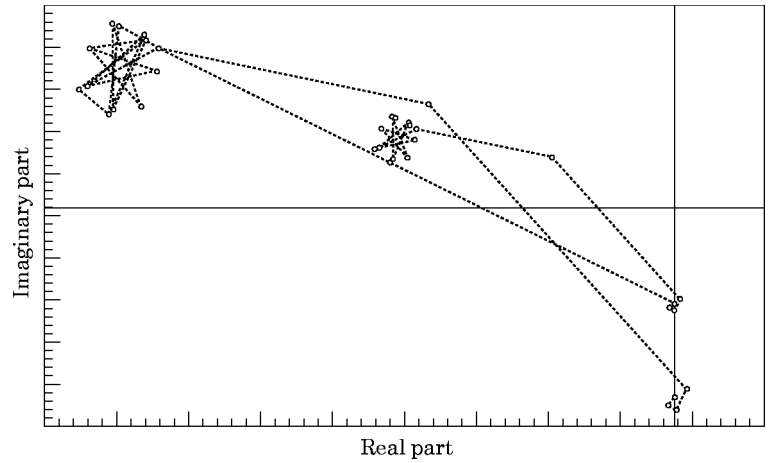

Figure 13. Test 1: the vector end of the complex envelope displacement in the complex plane.

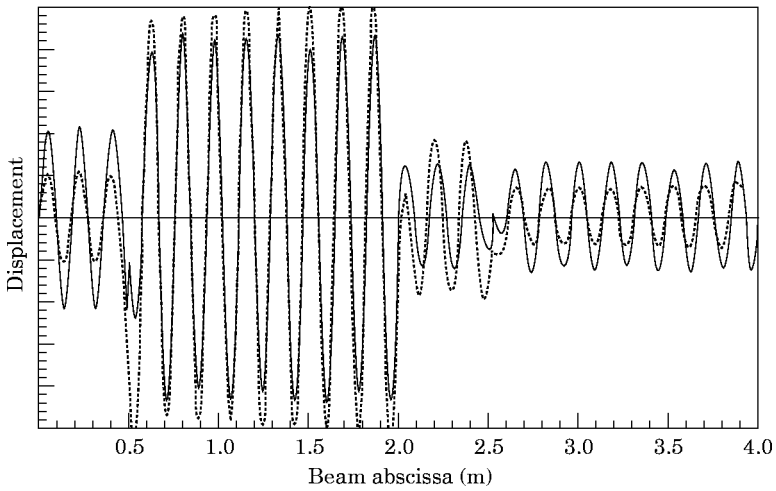

Figure 14. Test 1: a comparison between the physical and recovered displacements. – – –, Exact solution; ——, CEDA solution.

$f_2 = 8000$ Hz. Let $w_1(w)$ and $w_2(x)$ be the demodulated solutions corresponding to F_1 and F_2 when applied separately; then the total response can be expressed by

$$w(x, t) = w_1(x) \cos \omega_1 t + w_2(x) \cos \omega_2 t,$$

but, for comparison, the root-mean-square solution is considered:

$$\bar{w}(x) = (\sqrt{2}/2)[w_1^2(x) + w_2^2(x)]^{1/2}.$$

The exact and CEDA solutions are shown in Figure 15 (30 versus 300 points).

The third case refers to two coupled beams with hinged ends and differing cross-sections (see Figure 16). Two harmonic forces of equal frequency ($f = 12\,000$ Hz) are applied to the system: their amplitudes are $F_1 = 1000$ N and $F_2 = 2000$ N respectively. It is very interesting to note that even in this complex case the reconstructed physical displacement

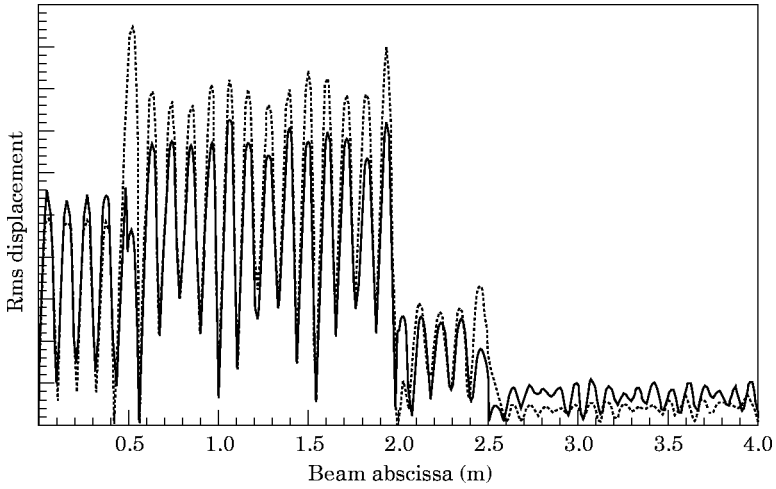

Figure 15. Test 2: a comparison between the physical and recovered displacements. Key as Figure 14.

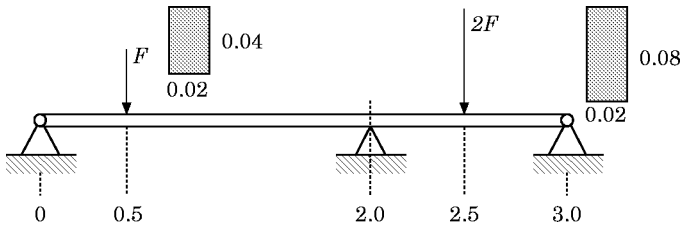

Figure 16. Simulated test 3: the dimensions of the beam.

matches the exact solution almost perfectly (Figure 17), although the envelope solution is obtained with 30 samples only against 400 samples for the exact one.

6. CONCLUSIONS AND PERSPECTIVES

A complex envelope displacement analysis, useful for dealing with medium and high frequency vibro-acoustic problems, has been presented here for one-dimensional flexural systems. The model is the natural evolution of previously developed envelope models, EEM and EPHEM [20], based on the concept of envelope energy density. This new formulation retains the main advantages of the mentioned approaches concerning the possibility of providing both the trend and the complete oscillating solution at low computational cost, but introduces some important improvements with respect to both the envelope approaches and the thermal methods. In particular, the forcing term of the governing equation is no longer the input power to the system that can be only roughly evaluated, but an expression directly related to the excitation force. Unlike EPHEM, which for flexural problems results in a pair of non-linear coupled equations for the envelope and the phase, the equation of this new model is linear and can be extended to more complex systems.

The most interesting property of the proposed approach relies on the quasi-static nature of the envelope solution, which can have interesting and attractive applications in vibro-acoustic problems and permits a low cost numerical computation; moreover, this does not prevent the possibility of reconstructing the oscillating response by simple

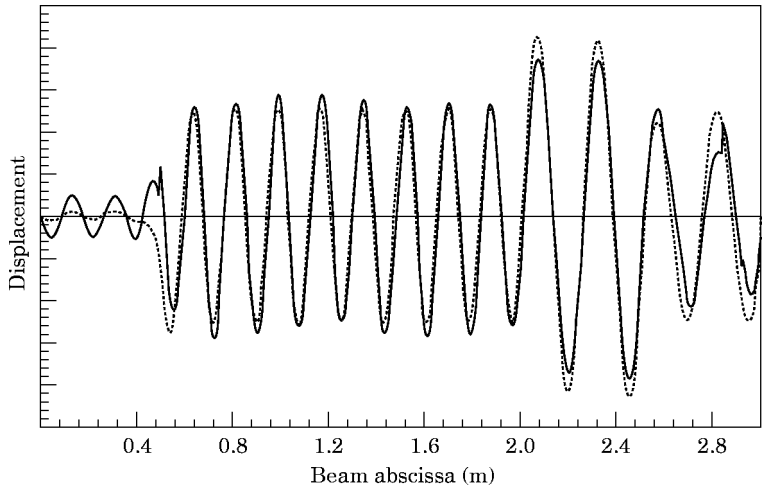

Figure 17. Test 3: a comparison between the physical and recovered displacements. – – –, Exact solution; ——, CEDA solution.

demodulation. Even if not necessary or convenient for further vibro-acoustic developments, it is a matter of fact that very often this possibility is of great importance. None of the previous proposed approaches provides this convenient property.

Another attractive application of the envelope solution could concern its use as a field descriptor related to the low wavenumber content of the response, linked to the radiating supersonic components of a vibrating structure. This point deserves careful analysis, but is likely to provide promising developments.

Although the method is particularly developed here for vibro-acoustic frequencies, it could be equally applied for any range of frequencies, because in the general formulation there is no restrictive hypothesis on the frequency. This is a relevant point because it is a matter of fact that both deterministic and statistical methods are unable to cover the whole range of interested frequencies, and a gap exists between the maximum frequency of the deterministic methods and the minimum frequency of the statistical ones, in which neither the former nor the latter are able to provide significant results.

In this paper, a detailed analysis of the proposed method has been presented, encompassing theoretical, practical and computational aspects; in particular, both the cases of narrow-band and wide-band displacement spectra have been considered, with exposition of their different solution schemes. The computational efficiency has been analyzed and discussed for different conditions.

Simulated results have been presented for simple and complex assembled beams to show the nature of the envelope solution.

ACKNOWLEDGMENTS

The authors wish to acknowledge Professors Fahy and Langley of the University of Southampton for their suggestions and co-operation during the visit, as a Ph.D. student, of Dr Carcaterra to the ISVR.

The present work has been supported partly by MURST through a 60% grant and partly by CNR (PFT2) through grant CT-01459.PF74.

REFERENCES

1. F. J. Fahy 1993 *Proceedings of Inter-Noise*, *Leuven*, Statistical energy analysis: a wolf in sheep clothing?
2. C. R. Fredö 1995 *Doctoral Thesis*, *Chalmers University of Technology*, *Göteborg*, Statistical Energy Analysis and the individual case.
3. B. R. Mace 1994 *Journal of Sound and Vibration* **178**, 95–112. On the SEA hypothesis of coupling power proportionality and some implications of its failure.
4. E. J. Skudrzyk 1980 *Journal of the Acoustical Society of America* **67**, 1105–1135. The mean value method of predicting the dynamic response of complex vibrations.
5. G. Maidanik and J. Dickey 1990 *Journal of Sound and Vibration* **139**, 31–42. Wave derivation of the energetics of driven coupled one-dimensional dynamic systems.
6. R. S. Langley 1992 *Journal of Sound and Vibration* **135**, 499–508. A general derivation of the SEA equations for coupled dynamic systems.
7. R. S. Langley 1989 *Journal of Sound and Vibration* **135**, 483–502. A wave intensity technique for the analysis of high frequency vibrations.
8. N. Lalor 1992 *ISVR Technical Report* **182**. Practical consideration for the measurement of internal and coupling loss factors.
9. L. E. Buvailo and A. V. Ionov 1980 *Soviet Physics—Acoustics* **26**, Application of the finite element method to the investigation of the vibro-acoustical characteristic of structures at high audio frequencies.
10. D. J. Nefske and S. H. Sung 1987 *ASME Publication NCA*-3: *Statistical Energy Analysis*. Power flow finite element analysis of dynamic systems: basic theory and application to beams.

11. J. D. Palmer, E. J. Williams and C. H. Fox 1993 *Proceedings of the 4th International Congress on Intensity Techniques*, *Senlis*, *France*, Energy flow analysis in built up structures.
12. M. Djimadoum and J. L. Guyader 1993 *Proceedings of the 4th International Congress on Intensity Techniques*, *Senlis*, *France*, Prediction of coupled beam energy with the equations of diffusion—boundary excitation and coupling conditions.
13. A. Le Bot 1994 *Ph.D. Dissertation*, *Ecole Central de Lyon*, *France*. Equations energetiques en mechanique vibratoire. Application au domain des moyennes at haute frequencies.
14. A. Carcaterra and A. Sestieri 1995 *Journal of Sound and Vibration* **188**, Energy density equations and power flow in structures.
15. A. Le Bot and L. Jezequel 1993 *Proceedings of the 4th International Congress on Intensity Techniques*, *Senlis*, *France*, Energy methods applied to transverse vibrations of beams.
16. A. Le Bot and E. Luzzato 1994 *Workshop on Methods in Medium and High Frequencies*. *An Alternative to SEA*, *Clamart*, *France*, Smooth energy formulation for multi-dimension problems.
17. A. Sestieri and A. Carcaterra 1995 *Journal of Sound and Vibration* **188**, 283–295. An envelope energy model for high frequency structural problems.
18. A. Carcaterra and A. Sestieri 1994 *Proceedings of the XIII International Modal Analysis Conference*, *Nashville*, Envelope versus envelope-phase energy model for high frequency vibrations.
19. A. Carcaterra and A. Sestieri 1994 *Proceedings of the 19th International Seminar on Modal Analysis*, *Leuven*, *Belgium*, Toward a complete definition of the envelope energy model for high frequency vibrations.
20. A. Sestieri and A. Carcaterra 1996 *Meccanica* **31**, 1–14. Circumventing space sampling limitations in mechanical vibrations.
21. R. S. Langley 1991 *Journal of Sound and Vibration* **150**, 47–66. Analysis of beam and plate vibrations by using the wave equation.
22. A. V. Oppenheim and R. W. Shafer 1975 *Digital Signal Processing*. Englewood Cliffs, NJ: Prentice-Hall.
23. R. N. Bracewell 1985 *The Fourier Transform and its Applications*. London: McGraw-Hill.

APPENDIX A: AN ALTERNATIVE DERIVATION OF THE COMPLEX ENVELOPE DISPLACEMENT EQUATION

Consider the two operators **L** and **H** defined above. It can be shown [19] that these operators commute: i.e., $\mathbf{H}[\mathbf{L}(\cdot)] = \mathbf{L}[\mathbf{H}(\cdot)]$. Applying the Hilbert transform to both sides of the equation of motion (1), one obtains

$$\mathbf{H}\{\mathbf{L}[w] + m\omega_0^2 w\} = \mathbf{H}\{p\},$$

so that, for the commutation property

$$\mathbf{L}[\tilde{w}] + m\omega_0^2 \tilde{w} = \tilde{p}. \tag{A1}$$

By combining equation (1) with equation (A1), the following equation is obtained in terms of the analytic displacement:

$$\mathbf{L}[\hat{w}(x)] + m(x)\omega^2 \hat{w}(x) = \hat{p}(x).$$

Now expressing the analytic displacement $\hat{w}$ in terms of the complex envelope displacement (equation (3)), one obtains

$$\mathbf{L}[\tilde{w}\, e^{jk_0 x}] + m\omega_0^2 \tilde{w}\, e^{jk_0 x} = \hat{p}.$$

Finally, upon multiplying each term by $e^{-jk_0 x}$, the complex envelope displacement equations is obtained as

$$\tilde{\mathbf{L}}[\tilde{w}] + m\omega_0^2 \tilde{w} = \tilde{p}, \tag{A3}$$

where the complex envelope operator is $\tilde{\mathbf{L}}(\cdot) = \mathbf{L}[(\cdot)\, e^{jk_0 x}]\, e^{-jk_0 x}$ equivalent to the definition given in section 2.2.

APPENDIX B: AN EXPLICIT FORM OF THE COMPLEX ENVELOPE EQUATION FOR FLEXURAL BEAMS

The equation of the Euler beam subjected to a harmonic load is given in the frequency domain by $w^{IV} - k_0^4 w = p/EI$. By applying the Hilbert transform to any term of this equation and adding this new equation to the equation of motion, one obtains

$$\hat{w}^{IV} - k_0^4 \hat{w} = \hat{p}/EI = \hat{q}, \tag{B1}$$

where $\hat{w}$ denotes the analytic displacement. Upon remembering that (from equation (3)) $\hat{w} = \tilde{w}\, e^{jk_0 x}$, it is straightforward to derive the complex envelope equation in terms of $\tilde{w}$. The subsequent derivatives of the analytic displacement are

$$\hat{w} = \tilde{w}\, e^{jk_0 x}, \qquad \hat{w}' = (\tilde{w}' + jk_0 \tilde{w})\, e^{jk_0 x},$$

$$\hat{w}'' = (\tilde{w}'' + 2jk_0 \hat{w}' - k_0^2 \tilde{w})\, e^{jk_0 x},$$

$$\hat{w}''' = (\tilde{w}''' + 3jk_0 \tilde{w}'' - 3k_0^2 \tilde{w}' - jk_0^3 \tilde{w})\, e^{jk_0 x},$$

$$\tilde{w}^{IV} = (\tilde{w}^{IV} + 4jk_0 \tilde{w}''' - 6k_0^2 \tilde{w}'' - 4jk_0^3 \tilde{w}' + k_0^4 \tilde{w})\, e^{jk_0 x}.$$

By substituting $\hat{w}^{IV}$ and $\hat{w}$ in equation (B1), one has

$$(\tilde{w}^{IV} + 4jk_0 \tilde{w}''' - 6k_0^2 \tilde{w}'' - 4jk_0^3 \tilde{w}' + k_0^4 \tilde{w}) - k_0^4 \tilde{w} = \tilde{q},$$

from which the structural envelope operator (7) is obtained. Therefore the complex envelope equation is given by $\tilde{\mathbf{L}}(\tilde{w}) - k_0^4 \tilde{w} = \tilde{q}$. By using Langley's approach [22], the fourth order equation is reduced to the second order far field equation

$$w'' + k_0^2 w = -p/2EIk_0^2 = q.$$

Upon writing the analytic displacement equation, and using the derivatives previously determined, the second order complex envelope equation becomes

$$(\tilde{w}'' + 2jk_0 \tilde{w}' - k_0^2 \tilde{w}) + k_0^2 \tilde{w} = \tilde{q}, \tag{B2}$$

so that the structural envelope operator is, for the second order equation,

$$\tilde{\mathbf{L}}(\cdot) = d^2(\cdot)/dx^2 + 2jk_0\, d(\cdot)/dx + k_0^2(\cdot).$$

After performing simplifications, the final form of the complex far field flexural displacement equation reduces to

$$\tilde{w}'' + 2jk_0 \tilde{w}' = \tilde{q}. \tag{B3}$$

APPENDIX C: THE FOURIER TRANSFORM OF A PARTICULAR SOLUTION

Here it is shown that

$$\tilde{w}_0(x) = -\tfrac{1}{2} \int_{-\infty}^{\infty} \frac{\tilde{P}(k)}{k(k + 2k_0)}\, e^{jkx}\, dk = \mathbf{E}(w_0):$$

i.e., it is the only part of the solution of equations (13) or (14) one is interested in. $w_0(x)$ is a particular solution of the Helmholtz equation, viz., $w_0'' + k_0^2 w_0 = p$. By Fourier transforming, one obtains

$$-k^2 W_0(k) + k_0^2 W_0(k) = P(k) \Rightarrow W_0(k) = P(k)/(k_0^2 - k^2).$$

The analytical signal that cancels the negative part of the spectrum yields $\widehat{W}_0(k) = \hat{P}(k)/(k_0^2 - k^2)$. Applying the envelope operator that shifts the positive part of the spectrum towards the origin of the k-axis, one has

$$\tilde{W}_0(k) = \widehat{W}_0(k + k_0) = \frac{\hat{P}(k + k_0)}{k_0^2 - (k + k_0)^2} = \frac{\tilde{P}(k)}{k(k + 2k_0)}.$$

Therefore $\tilde{W}_0(k)$ is the complex envelope spectrum of a particular solution of the physical motion equation. By inverse transforming into space,

$$\tilde{w}_0(x) = -\tfrac{1}{2} \int_{-\infty}^{\infty} \frac{\tilde{P}(k)}{k(k + 2k_0)} \, \mathrm{e}^{\mathrm{j}kx} \, \mathrm{d}k,$$

which shows that the first term of the general solution of the envelope equation exactly corresponds to the complex envelope of a particular solution of the physical equation.

It is easy to verify that this is a low wavenumber signal due to the same nature of $\tilde{P}(k)$ (nil for $k < -k_0$) and to the factor $1/k(k + 2k_0)$ that concentrates the energy around k_0.